Journal of Inflammation Research

Dovepress
Taylor & Francis Group

Open Access Full Text Article

ORIGINAL RESEARCH

Interleukin Family-Based Signature Relates to Cancer-Associated Fibroblasts Spatial Distribution and Immune Therapy Response in Pancreatic Carcinoma

Yang Cheng[1,2,*], Shuzhe Xiao[3,*], Xiangzhao Li[4,*], Biao Wang[5], Yi Lei[1], Penghui Sun[6], Li Ma[2], Yun Zhu[1]

[1]Department of Infectious Diseases, Nanfang Hospital, Southern Medical University; State Key Laboratory of Organ Failure Research; Key Laboratory of Infectious Diseases Research in South China, Ministry of Education; Guangdong Provincial Key Laboratory for Prevention and Control of Major Liver Diseases; Guangdong Provincial Clinical Research Center for Viral Hepatitis; Guangdong Institute of Hepatology; Guangdong Provincial Research Center for Liver Fibrosis Engineering and Technology, Guangzhou, Guangdong, 510515, People's Republic of China; [2]Digestive Department, Guangzhou Women and Children's Medical Center, Guangzhou Medical University, Guangzhou, Guangdong, 510623, People's Republic of China; [3]Department of Neonatology, Nanfang Hospital, Southern Medical University, Guangzhou, Guangdong, 510515, People's Republic of China; [4]Department of Pathology, Nanfang Hospital, Southern Medical University, Guangzhou, Guangdong, 510515, People's Republic of China; [5]Department of Hepatobiliary Surgery, Nanfang Hospital, Southern Medical University, Guangzhou, Guangdong, 510515, People's Republic of China; [6]Nanfang PET Center, Nanfang Hospital, Southern Medical University, Guangzhou, Guangdong, 510515, People's Republic of China

*These authors contributed equally to this work

Correspondence: Yun Zhu, State Key Laboratory of Organ Failure Research, Guangdong Provincial Key Laboratory for Prevention and Control of Major Liver Diseases, Department of Infectious Diseases, Nanfang Hospital, Southern Medical University, Guangzhou, Guangdong, 510515, People's Republic of China, Email zyfreemail@126.com

Background: Cancer-associated fibroblasts (CAFs) and interleukins (ILs) family play crucial roles in pancreatic carcinoma (PC) immune response. However, the correlation between the IL family, CAFs infiltration, and PC prognosis remains uninvestigated.

Methods: An IL family expression pattern for prognosis was constructed using a stepwise Cox proportional hazards regression model using TCGA data. Clinical data and validations from seven independent public cohort datasets were conducted to confirm the performance of the model. CAFs infiltrating abundance and spatial distribution in PC, and their correlation with patient prognosis were detected. Correlation between IL expression pattern, CAF infiltration, and immunotherapy response was evaluated using clinical tissue samples.

Results: This study constructed the first IL family expression pattern to predict CAFs infiltration and prognosis in PC. The model was validated using clinical data and a meta-analysis of seven public PC datasets (HR= 1.27). IL high-risk patients had shorter survival, advanced tumors and lymph node metastasis compared to low-risk patients. Patients with unfavorable immunotherapy response had significantly higher IL risk scores (P=0.015). The IL expression pattern distinguished CAFs infiltration characteristics in PC, showing greater infiltration of CAFs, antigen-presenting CAFs (apCAFs) and inflammatory CAFs in the high-risk group. IL high-risk group also exhibited increased apCAF/tumor cell and apCAF/Tregs engagement, resulting in suppressed immune responses, crippled T-cell function and B-cell function, and elevated levels of biomarkers associated with poor immune response.

Conclusion: This study constructed the first IL expression pattern related to CAFs infiltration, immunotherapy response, and prognosis in PC patients. This might promote precise immunotherapy and facilitate treatment options for PC.

Keywords: pancreatic carcinoma, IL family, cancer-associated fibroblasts infiltration, immunotherapy response, prognosis

Introduction

The incidence and mortality of pancreatic carcinoma (PC) are increasing annually.[1,2] Immunotherapy, while crucial in cancer treatment, is less effective for PC, showing higher resistance to immune checkpoint inhibitors(ICIs) compared to

Received: 2 May 2025
Accepted: 21 July 2025
Published: 29 July 2025

other tumors.[3] Clinical research shows that ICIs treatment does not improve the survival rates of patients with advanced PC.[4] The mechanisms behind this poor response remain unclear.

Cancer associated fibroblasts (CAFs) are involved in intricate crosstalk with cancer cells and immune cells, playing a critical role in PC progression.[5] CAFs exhibit significant functional heterogeneity within the PC tumor microenvironment. Exploring the heterogeneity and spatial distribution of CAFs in the PC will provide important insights into the complex and heterogeneous immune landscape associated with progression.

Predictive biomarker studies have achieved success in other solid tumors, but findings remain limited in PC. A precision predictor is needed to forecast prognosis and match effective therapies to immune microenvironmental characteristics. Interleukins (ILs), cytokines produced by a variety of tissue and blood cells, play significant roles in the inflammatory response during various infectious diseases. They are also key cytokines that regulate immune cell activation and tumor immune responses, playing a critical role in the development and progression of PC.[6] Different IL members exert distinct regulatory effects on tumor immunity,[7] with some abnormally expressed in PC.[8,9] A better understanding of the IL family profile and the clinical characteristics as well as immunological characteristics in PC could optimize cancer treatment.

In the current study, an IL expression signature that is related to PC prognosis was established through comprehensive analysis of prognostic data and IL family expression in clinical tissue samples and genomics data from databases such as the Cancer Genome Atlas (TCGA). For the first time, the relationship between IL family expression and CAFs infiltration and spatial distribution in PC were explored. Additionally, the potential predictive value of this IL expression signature for immunotherapy response was evaluated.

Materials and Methods

Construction of IL Family-Based Signature and Prognostic Analysis in TCGA Dataset

Data of IL family mRNA expression, clinicopathological characteristics, and overall survival (OS) data of patients of TCGA PAAD database were used (Supplementary Table S1). Univariate Cox proportional hazards regression analysis was used to evaluate the relationship between IL family member gene expression and OS in PC patients. Variables with a P-value< 0.05 were subsequently incorporated in the multivariate model. A stepwise Cox proportional hazards regression model was performed to screen for the most predictive gene markers. The stepwise multivariable Cox regression was performed using the 'My.stepwise' package for R. The selected genes formed a risk-assessment score based on a linear combination of gene-expression levels.

Model Validation in Public Databases

IL family mRNA expression levels and OS data in PC patients were obtained from the International Cancer Genome Consortium (ICGC) database (80 patients) and Gene Expression Omnibus (GEO) datasets, including GSE21501 (102 patients), GSE57495 (63 patients), GSE62452 (66 patients), GSE71729 (125 patients), and GSE79668 (51 patients). There are no significant differences in ethnicity, age distribution, or tumor subtype composition among the five GEO databases. The overall hazard ratio (HR) was calculated using a random-effects model.

Clinical Samples and Immunohistochemistry

Surgically resected tumor tissues and adjacent normal tissues were collected from 90 patients with PC (Shanghai Outdo Biotech, Shanghai, China). Patient characteristics are shown in Table 1.

Microarray chips of samples were stained with anti-IL1R2, anti-IL4, anti-IL8, anti-IL13RA2, anti-IL20RA, anti-IL20RB, anti-IL27 (Abbkine, Wuhan, China), anti-IL1RN, anti-IL6R, and anti-IL18 (Affinity Biosciences, Cincinnati, OH, USA USA) as previously described.[10] The staining score was independently assessed by two researchers.

Microarray chips were stained with anti-Ki67 (Abbkine, Wuhan, China) and anti-P53 (Abcam, Cambridge, UK) antibodies. The p53 status was determined by the percentage range of stained tumor cell nuclei as previously described.[11] Specifically, cases with p53-stained nuclei exceeding 20% of total tumour cell or completely absent in tumour cells were categorized as "p53-positive".

Table 1 Characteristics of the Clinical PC Patients

Variable	No. of Patients
Age, yr	
Median	62
Range	34-83
Age group, no. (%)	
<65	52(58)
≥65	38(42)
Sex, no(%)	
Male	58(64)
Female	32(36)
Pathological grade, no. (%)	
I/II	58(65)
II–III	21(23)
III–IV	11(12)
TNM Staging(T), no. (%)	
T1	2(2)
T2	72(80)
T3	16(18)
TNM Staging(N), no. (%)	
N0	51(57)
N1	39(43)
TNM Staging(M), no. (%)	
M0	89(99)
M1	1(1)

Survival Analysis for Clinical PC Patients

Patients were divided into high- and low-risk groups according to the optimal cut-off value using the constructed risk-prediction model. Survival analysis was conducted using Kaplan–Meier survival estimates. Univariate and multivariate Cox regression analyses were performed for survival analysis of clinical characteristics of patients, including sex, age, metastasis, pathological grade, and IL risk model.

Multiplex Fluorescent Immunohistochemistry Staining and Cell-to-Cell Distance Analysis

Formalin-fixed, paraffin-embedded sections were dewaxed and dehydrated, then peroxide-blocked. The Opal seven-color manual immunohistochemistry kit (PerkinElmer, Waltham, MA, USA) was used, following the manufacturer's instructions. The slides were incubated with the primary antibody for 1 hour, followed by incubation with secondary antibody

for 10 minutes. The slides were then incubated in Opal dye diluent (diluted 1:100) for 10 minutes. After each step, the slides were thoroughly washed with TBST buffer. Microwave treatment was used to remove the primary and secondary antibodies prior to counterstaining. These steps were repeated until all indicators were labeled. Finally, the slides were incubated with the DAPI working solution for 5 minutes and mounted using a fluorescence anti-quenching medium.

The primary antibodies used are as follows: Cancer Associated Fibroblast Marker Antibody Sampler Kit, anti-PDPN, anti-FoxP3 (Cell Signaling Technology, Danvers, MA, USA), and anti-KRT8 (Abcarta, Suzhou, China). Slides were scanned to obtain seven-colored, whole-slide images using TissueFAXS Spectra S (TissueGnostics GmbH, Vienna, Austria). Image analysis was completed with TissueGnostics StrataQuest (TissueGnostics GmbH, Vienna, Austria). CAF were defined as $PDPN^+$, antigen-presenting CAF (apCAF) were defined as $PDPN^+$ $CD74^+$, inflammatory CAFs (iCAFs) were defined as $PDPN^+$ $PDGFRA^+$, and regulatory T-cells (Tregs) were defined as $Foxp3^+$, respectively. Multiplex fluorescent composite images were reviewed by pathologists to confirm the accuracy of staining and phenotyping. The distance between a cell and its nearest neighbors and the number of cells connected to other cells within a set radius were calculated using R (R Foundation for Statistical Computing, Vienna, Austria).

Immunofluorescence staining of tissue sections was performed as described before,[12] antibody against anti–programmed death-ligand 1 (PD-L1) (Gene Company Ltd., Hong Kong) was used.

IL Expression Pattern and Immune Cell Infiltration Evaluation in PC Patients with Different Immunotherapy Response

Formalin- fixed, paraffin-embedded (FFPE) blocks were collected from five patients with favorable PD-1 antibody therapy effect and five patients with unfavorable PD-1 antibody therapy effect at the Nanfang Hospital, between January 1, 2019 and January 31, 2023.

IHC for IL family and multiplex fluorescent immunohistochemistry staining for indicated proteins were performed.

Immune Cell-Infiltration Analysis

The pattern of immune cell infiltration between the high- and low-risk groups was estimated by CIBERSORT, a novel method widely used for characterizing the infiltrating immune cell composition in tumors.[13] The LM22 signature algorithm, which contains 547 genes to distinguish 22 immune cell subtypes was used.

Biological Process and Pathway Enrichment Analysis

Gene Ontology (GO) and Kyoto Encyclopedia of Genes and Genomes (KEGG) pathway enrichment analysis were applied using DAVID to explore the biological functions and pathways of the related genes.

Quantification of the Immune Response Predictor

The numbers of neo-antigens, clonal and subclonal neo-antigens in PC patients in the TCGA dataset were obtained through The Cancer Immunome Atlas (https://tcia.at/home).[14] A reverse-phase protein array analysis was performed to quantify the expression of PD-L1 from the TCGA dataset, which was retrieved from the cBio Cancer Genomics Portal (http://www.cbioportal.org). The Tumor Immune Dysfunction and Exclusion (TIDE) platform integrates T-cell dysfunction and exclusion signatures to evaluate tumor immune evasion and predict the immune checkpoint inhibitor response.[14]

Statistical Analysis

Statistical analyses were performed with GraphPad Prism version 6.0 (GraphPad Software, San Diego, CA, USA). The STATA software program (StataCorp LLC, College Station, TX, USA) was used for prognostic meta-analysis. An unpaired test was performed to detect differences between two groups. Random Forest Survival Analysis (RFSA) from machine learning was employed to validate the importance of the risk score genes using R (version 4.4.0) with package "random Forest SRC" and "survival". The survminer package in R was utilized to determine the optimal cut-off value.

Results

Construction of the IL Family-Based Signature and Its Correlation with Clinical Features

We intended to explore the correlation between IL family expression characteristics and PC prognosis. We analyzed 43 IL family genes, focusing on their association with OS of 178 patients in the TCGA PAAD cohort using univariate analyses. Ten genes were significantly associated with OS (Table 2): Seven were risk factors (*IL27, IL1RN, IL1R2, IL18, IL20RB, IL8*, and *IL20RA*) and three were protective factors (*IL4, IL13RA2*, and *IL6R*). The 10 selected genes were used to build a risk-prediction model for PC prognosis. The risk score is as follows: − 0.0697**IL13RA2* + 0.2527**IL18* +

Table 2 Univariate Analyses of IL Family Members with OS in the TCGA PAAD Cohort

Gene	HR	95% CI	p Value
CD4	1.027	0.864–1.22	0.766
IL10	1.022	0.672–1.552	0.92
IL10RA	0.896	0.739–1.087	0.266
IL10RB	1.387	0.978–1.967	0.066
IL12RB1	1.13	0.861–1.484	0.379
IL12RB2	1.375	0.837–2.259	0.208
IL13	0.183	0.028–1.182	0.074
IL13RA1	1.104	0.788–1.545	0.566
IL13RA2	0.724	0.562–0.933	0.013
IL16	0.951	0.807–1.119	0.543
IL17A	0.857	0.007–108.723	0.95
IL17F	0.243	0.002–25.17	0.55
IL17RA	1.155	0.75–1.778	0.512
IL17RC	0.826	0.572–1.192	0.307
IL18	1.562	1.228–1.988	< 0.001
IL18R1	0.913	0.688–1.211	0.526
IL18RAP	0.878	0.566–1.363	0.563
IL19	1.141	0.631–2.064	0.662
IL1A	1.08	0.871–1.34	0.483
IL1B	1.027	0.842–1.254	0.79
IL1F10	32.418	0.024–43,287.451	0.343
IL1R1	1.178	0.985–1.408	0.072
IL1R2	1.236	1.083–1.41	0.002
IL1RN	1.32	1.142–1.526	< 0.001
IL2	0.395	0.112–1.391	0.148

(*Continued*)

https://doi.org/10.2147/JIR.S532651

Table 2 (Continued).

Gene	HR	95% CI	p Value
IL20RA	1.358	1.037–1.778	0.026
IL20RB	1.358	1.191–1.549	< 0.001
IL21	0.483	0.022–10.706	0.646
IL21R	1.042	0.804–1.35	0.755
IL23A	1.187	0.945–1.492	0.141
IL23R	0.508	0.092–2.8	0.437
IL26	0.488	0.026–9.127	0.631
IL27	4.258	1.265–14.333	0.019
IL27RA	0.996	0.751–1.322	0.979
IL2RA	1.137	0.949–1.363	0.164
IL4	0.075	0.011–0.522	0.009
IL4R	1.281	1–1.641	0.05
IL6	1.077	0.95–1.22	0.249
IL6R	0.773	0.624–0.956	0.018
IL6ST	1.023	0.812–1.29	0.847
IL8	1.153	1.025–1.295	0.017
CXCR1	1.089	0.8–1.483	0.587
CXCR2	1.079	0.806–1.445	0.609

Abbreviations: HR, hazard ratio; CI, confidence interval.

$0.1663*IL1R2 - 0.04*IL1RN + 0.2286*IL20RA + 0.2153*IL20RB + 0.9383*IL27 - 2.5173*IL4 - 0.1782*IL6R - 0.0177*IL8$. Supplementary Figure S1 showed that the results of the RFSA indicate that these 10 genes are important for predicting patient survival outcomes (variable importance greater than 0 indicated by a blue bar). The Supplementary Figure S2 showed that both models perform similarly and both are close to the reference line.

The distributions of risk score, survival status, and gene-expression panel are shown in Figure 1A and B. Patients in the TCGA dataset were divided into high-risk (n = 35) and low-risk (n = 143) groups based on the optimal cutoff value. High-risk patients had significantly shorter OS compared to low-risk patients (Supplementary Figure S3A). This trend was consistent across early-stage (stages I and II) and late-stage (stages III and IV) subgroups (Supplementary Figure S3B and C). This indicates that the risk score effectively distinguished between improved and poor prognoses. Cox regression analyses indicated that the IL family–based signature independently correlates with OS in PC patients (Table 3).

The predictive ability of the IL family signature was evaluated in clinical PC patients. Expression levels of the indicated IL family members in tumor and normal tissues are shown in Figure 1C. Clinical PC patients were divided into high- and low-risk groups based on their formula scores. The low-risk group contained a greater proportion of patients with low pathological grades, while the high-risk group had more patients with high pathological grades (Figure 1D). Moreover, the high-risk group had significantly more lymph node metastases (Figure 1E) and shorter OS times (Figure 1F). High-risk patients also exhibited greater tumor-proliferation ability, as indicated by Ki67 expression (Figure 1G), a higher proportion of p53 mutations (Figure 1H), and a greater percentage of PD-L1–positive cells

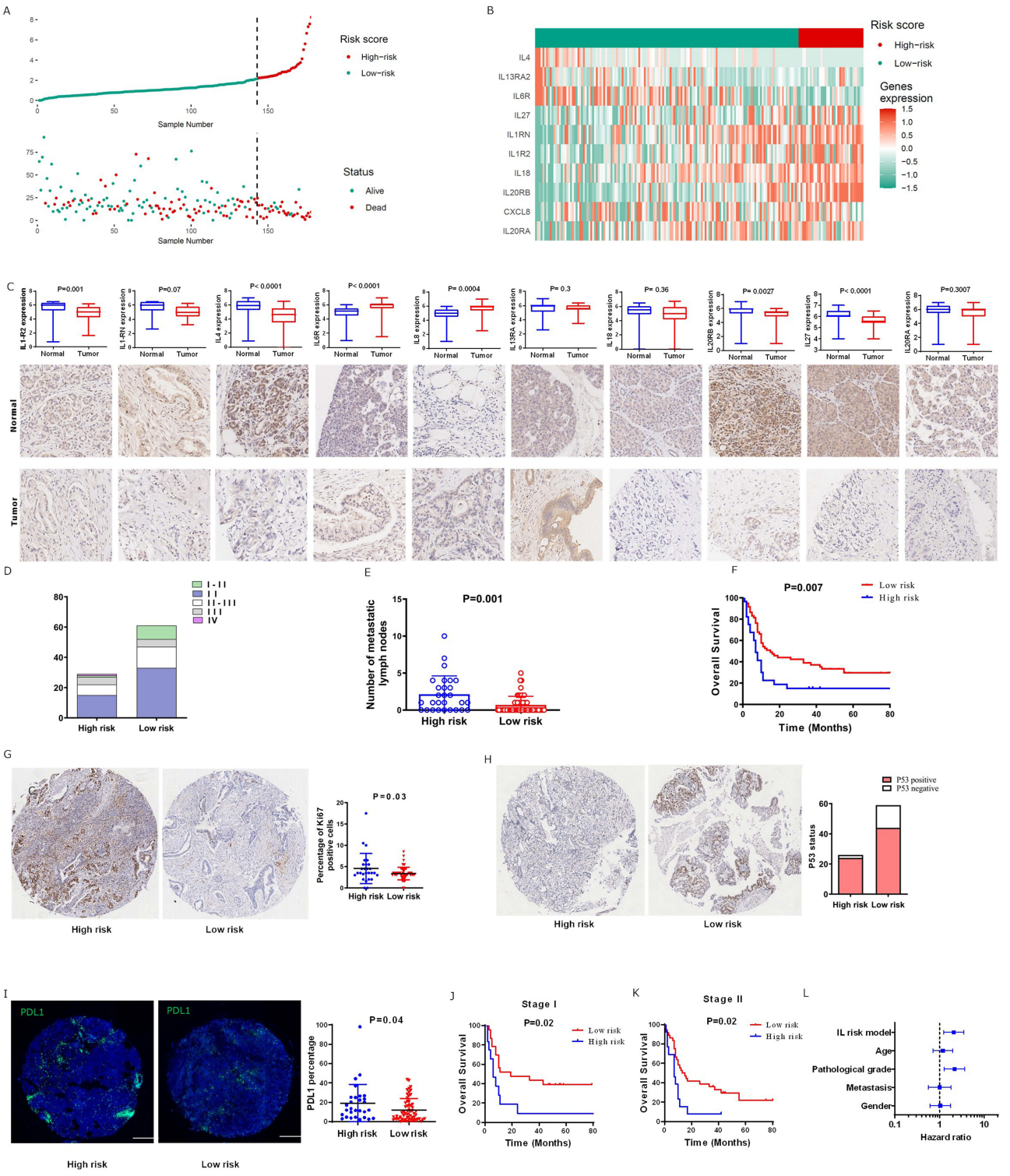

Figure 1 The prognostic performance of the IL family–based signature in the clinical cohort. **(A)** IL family gene expression–based distribution of risk score and survival status of patients in the TCGA dataset. (**B**) Heatmap of the expression of the 10 IL family genes forming the prognostic risk model in the TCGA dataset. (**C**) The expression of ILs in PC and normal tissues. (**D**) Distribution of the pathological grade of clinical cohort patients (n = 90) in high- and low-risk groups. (**E**) Number of metastatic lymph nodes of clinical cohort patients in the high- and low-risk groups. (**F**) Kaplan–Meier curves of OS for clinical PC patients in the high- and low-risk groups. (**G**) The proportion of Ki67-positive cells, p53 status (**H**), and the percentage of PD-L1–positive cells (**I**) in tumor tissues of both groups. Typical pictures of PD-L1 expression are shown. Bar = 250 μm. (**J**) Kaplan–Meier curves for OS in stage I and stage II tumors (**K**) in high- and low-risk groups. (**L**) Multivariate analysis of IL family risk score and clinical factors for prognosis prediction.

https://doi.org/10.2147/JIR.S532651

Table 3 Univariate and Multivariate Analyses of Risk Score and Clinicopathological Characteristics with OS in the TCGA PAAD Cohort

Characteristics	HR (95% CI)	p Value	HR (95% CI)	p Value
IL risk score	1.584 (1.406–1.785)	<0.001	1.542 (1.358–1.75)	<0.001
Age	1.028 (1.007–1.049)	0.01	1.024 (1.003–1.045)	0.026
Gender	0.813 (0.541–1.222)	0.319		
Pathological grade	1.532 (0.993–2.363)	0.054		
Stage	0.402 (0.127–1.273)	0.121		
Pathologic_T	2.035 (1.079–3.838)	0.028	1.256 (0.634–2.485)	0.513
Pathologic_M	0.773 (0.185–3.227)	0.724		
Pathologic_N	2.161 (1.287–3.627)	0.004	1.727 (0.986–3.024)	0.056

Abbreviations: CI, confidence interval; HR, hazard ratio; IL, interleukin.

Table 4 Univariate and Multivariate Analyses of Factors Associated with OS in Clinical Samples

Variables	Univariate	Multivariate	
	p Value	HR (95% CI)	p Value
Pathological grade (I–II/III–IV)	0.006	2.17 (1.28–3.67)	0.003
Gender (female/male)	0.556	1.04 (0.61–1.77)	0.893
Metastasis (no/yes)	0.824	1.01 (0.56–1.82)	0.982
Age, years (≤60/>60)	0.532	1.18 (0.71–1.96)	0.516
IL score (low/high)	0.007	2.08 (1.23–3.51)	0.006

Abbreviations: CI, confidence interval; HR, hazard ratio; IL, interleukin.

(Figure 1I). Subgroup analysis showed that stage I or II high-risk patients had significantly shorter OS (Figure 1J and K). Multivariate analysis showed that the IL family risk score is an independent predictor of prognosis in clinical PC patients (Figure 1L and Table 4). These results indicated that the IL family–based signature can effectively differentiate high- and low-risk PC patients and predict their prognosis.

Validation of the IL Family-Based Signature Using Multiple Independent Cohorts

We further validated the reproducibility of the prognostic value of the IL family–based signature in PC patients in five independent GEO data sets and one ICGC cohort. Patients in each cohort were divided into high- and low-risk groups according to the formula score based on the optimal risk value cutoff point. Kaplan–Meier analyses showed that the high-risk group had significantly lower OS compared to the low-risk group in GSE21501 (Figure 2A), GSE57495 (Figure 2B), and PACA (Figure 2C). Conversely, the high-risk group had significantly longer OS times in GSE71729 (Figure 2D). No significant difference in OS existed between the two groups in GSE62452 or GSE79668 (Figure 2E and F). Furthermore, a meta-analysis was conducted to evaluate the prognostic significance of the IL family–based signature in the seven public cohorts from the TCGA, GEO, and ICGC datasets (n = 665). Our results confirmed that the IL family–based signature is a risk factor for patients with PC (combined HR, 1.27; 95% confidence interval, 1.05–1.55; meta-analysis p = 0.016) (Figure 2G).

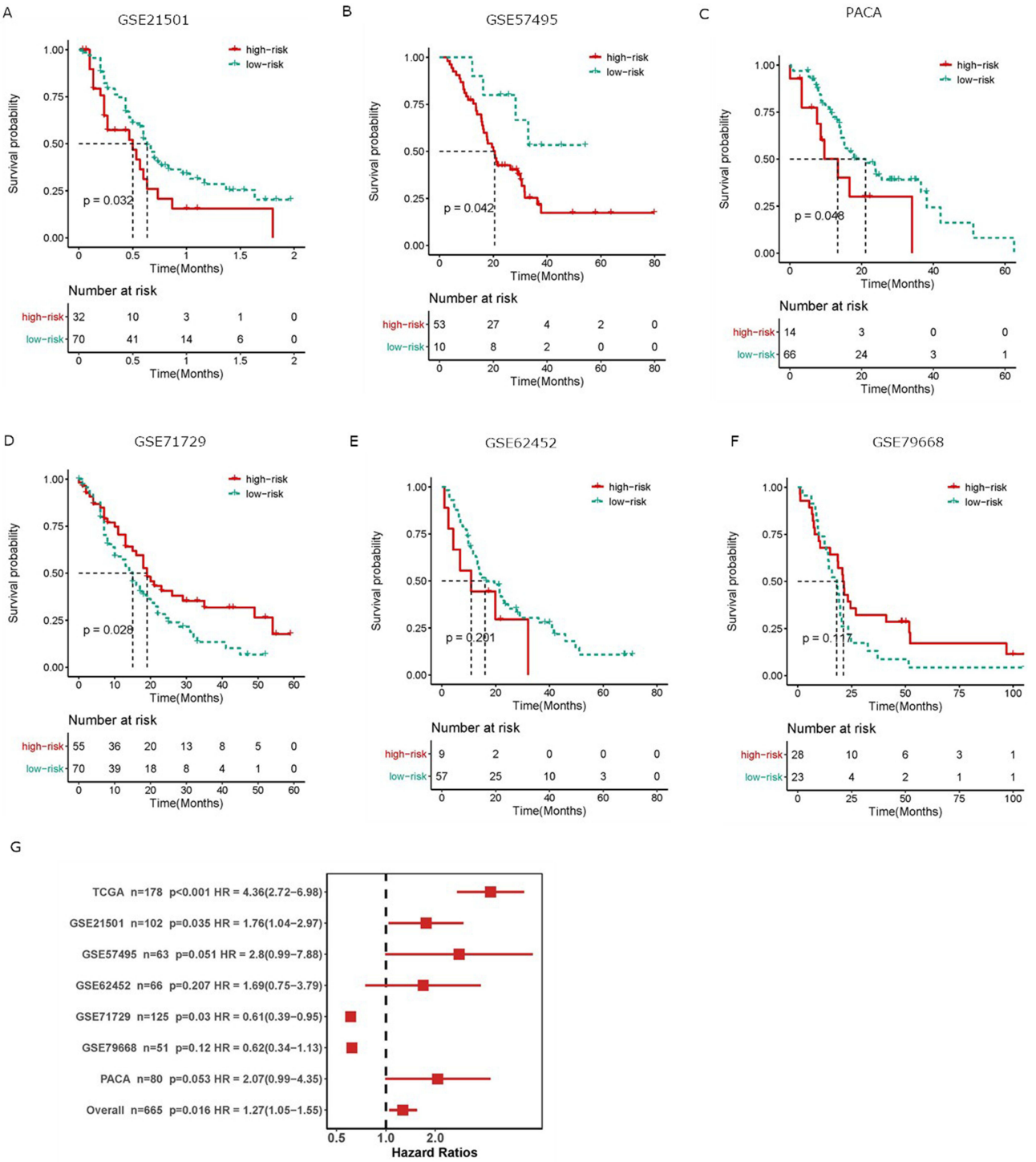

Figure 2 IL family–based signature and prognosis of PC in datasets. (**A**) Kaplan–Meier curves of OS for GSE21501, (**B**) GSE57495, (**C**) GSE62452, (**D**) GSE71729, (**E**) GSE79668, and (**F**) PACA. (**G**) Forest plot showing the meta-analysis results from TCGA, GEO, and ICGC datasets.
Abbreviation: HR, hazard ratio.

Infiltration Characteristics of CAFs in PC Correlate with Prognosis

We explored the correlation between the CAFs characteristics in the tumor immune microenvironment and PC prognosis. The infiltration of CAFs, apCAF, inflammatory CAF (iCAF), and Tregs in PC tissue (n = 90) was explored using a novel tyramide signal amplification (TSA) multiplex fluorescent immunohistochemistry staining approach. We simultaneously

https://doi.org/10.2147/JIR.S532651

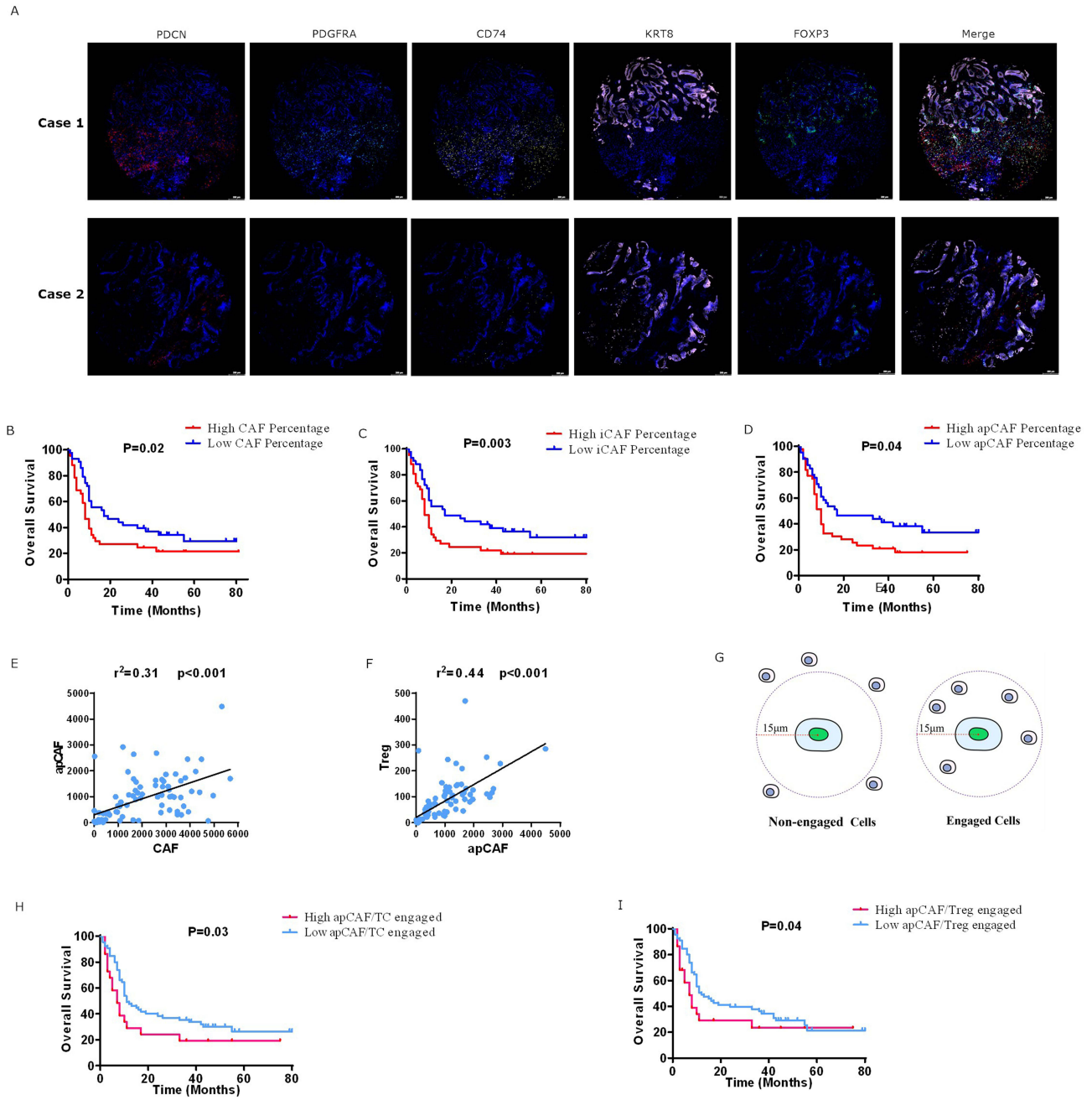

Figure 3 Infiltration abundance and spatial distribution of immune cells in tumor tissue and prognosis of clinical PC patients. (**A**) Multiplex fluorescent immunohistochemistry of PC patients in the clinical cohort (n = 90). Typical composite images are presented. Case 1, poor prognosis (OS, 11 months). Case 2, favorable prognosis (OS, 58 months). (**B**) Survival curves of patients with high/low CAFs, iCAFs (**C**), and apCAFs (**D**) in tumor tissue. (**E**) Correlation between CAFs and apCAFs infiltration. (**F**) Correlation between apCAFs and Tregs infiltration. (**G**) Schematic of engaged and non-engaged cells based within a 15 μm radius from the nucleus center. (**H**) Survival curves of PC patients with high/low apCAF engagement with tumor cells and Tregs (**I**). TC, epithelial tumor cells.

evaluate seven cell surface markers in 90 PC tissue samples (Figure 3A). High infiltration of CAFs, apCAFs, and iCAFs correlated with poor patient prognosis (Figure 3B–D). CAF levels positively correlated with apCAF levels (Figure 3E, R^2=0.31, p<0.001), and Treg proportions positively correlated with apCAF levels (Figure 3F, R^2=0.44, p<0.001).

To investigate the spatial distribution characteristics of CAFs in PC tissue, the distances between CAFs and tumor cells/ Tregs were measured. Cells with a distance of less than 15 μm from the nucleus to neighboring cells were considered to be engaged, while those over 15 μm apart were non-engaged[15] (Figure 3G). Figure 3H–I showed that

patients with lower engagement between apCAFs and tumor cells or Tregs had better prognosis. The results suggest that CAF infiltration and spatial distribution can serve as prognostic predictors.

The IL Family-Based Signature Distinguishes CAFs Infiltration and Spatial Distribution in the PC Microenvironment

The association between IL risk score and CAFs characteristics in clinical PC samples was explored. Multiplex fluorescent immunohistochemistry staining showed that patients in the low-risk group had significantly fewer CAFs, iCAF, and apCAFs in the tumor samples compared to the high-risk group (Figure 4A–D). Moreover, the low-risk patients had significantly lower Treg infiltration (Figure 4E). These results confirm the IL signature could effectively distinguish CAFs and Tregs infiltration in PC, supporting its prognostic value.

The value of the IL-based signature in distinguishing the spatial distribution characteristics of CAFs in PC tissues was detected. Our study showed higher apCAF and tumor cell engagement in the high-risk group (Figure 4F), as well as higher apCAF and Treg engagement in the tumor microenvironment of the high-risk group (Figure 4G). These results

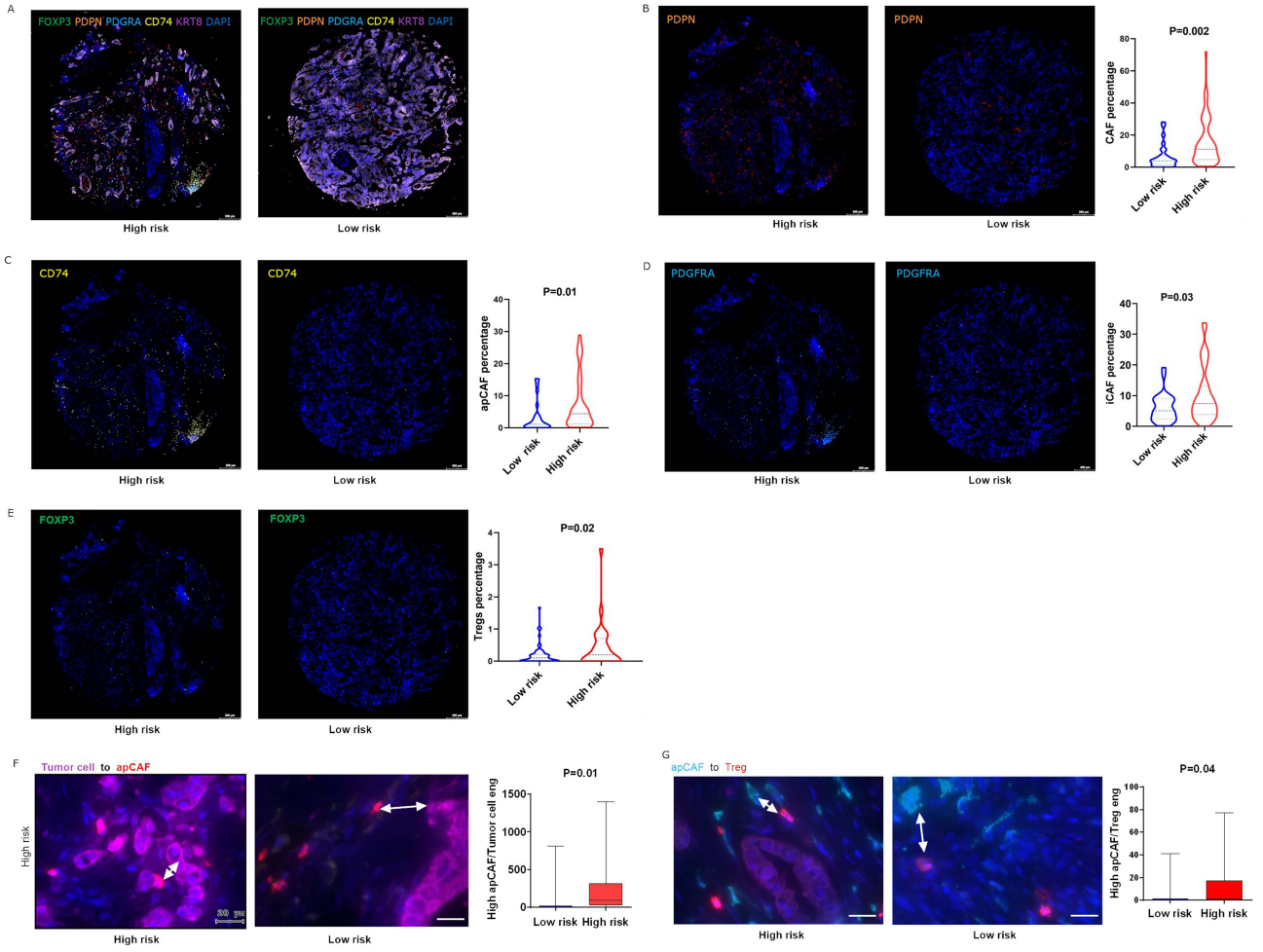

Figure 4 IL family–based signature associated with the abundance and spatial distribution of infiltrated immune cells. (**A**) Typical composite images from multiplex fluorescent immunohistochemistry in the IL high- and low-risk groups. (**B**) Proportions of total CAFs, apCAFs (**C**), iCAFs (**D**), and Tregs (**E**) in tumor tissue in high- and low-risk groups. Single fluorophore images show PDPN^{+}/CD 74^{+}/PDGFRA^{+} /FOXP3^{+} cells. Bar = 250 μm. (**F**) Number of apCAFs within 15 μm from the nuclear center of epithelial tumor cells in the high- and low-risk groups (right). Typical images are shown (left). Red represents apCAFs and purple represents tumor cells. (**G**) Number of highly engaged apCAFs and Tregs in high- and low-risk groups. Blue represents apCAFs and red represents Tregs. Arrow, the spatial separation between the two types of cells. Bar = 20 μM.

https://doi.org/10.2147/JIR.S532651

suggest that the IL family–based signature is associated with apCAFs and tumor cells/Tregs engagement, serving as a prognostic indicator.

IL Expression Pattern and CAFS Infiltration Signature in PC Patients with Favorable Immunotherapy Response

We identified a cohort of PC patients who received immune checkpoint blockade (ICB), and had evaluable imaging at our institution. Through radiographic quantitation of tumor burden, we categorized patients into favorable responders and unfavorable responders. To confirm the predictive efficacy of IL risk score in immunotherapy, we evaluated IL risk score between five favorable responders and unfavorable responders with available tissues. While single interleukin expression showed no significant (Figure 5A and B, Supplementary Figure S4), the IL risk score clearly distinguished the two groups. Favorable responders exhibited significantly lower scores while unfavorable responders had higher scores (Figure 5C). Additionally, favorable responders exhibited significantly reduced CAFs and apCAFs infiltration in tumor tissue compared to unfavorable responders (Figure 5D). Lower engagement of apCAF with tumor cells and Tregs was also observed in favorable responders (Figure 5E). These results suggest that the IL –based signature can immunotherapy response in PC.

Immune Profile and Immunotherapy Response Markers Related to the IL Family-Based Signature

To elucidate the IL family–based signature–related biological role, genes closely related to IL risk scores in the TCGA cohort were identified (Pearson $|r| > 0.4$). GO and KEGG analyses revealed enrichment in focal adhesion, p53 signaling, and PI3K/Akt signaling pathways (Figure 6A and B). The relationship between the IL family–based signature and tumor infiltration of 22 immune cell types was estimated using CIBERSORT (Figure 6C). The high-risk group had significantly fewer monocytes and more M0 macrophages compared to the low-risk group (Figure 6D–F).

Immune system–related metagene clusters may predict prognosis in cancers.[16] To better understand the risk score–related immune response, the association between risk score and immune system–related metagene clusters was explored. The heatmap for the expression of these metagenes in the TCGA PAAD cohort is shown in Figure 6G. Gene set variation analysis was used to detect the correlation between changes in the seven metagene clusters and the risk score.[17] Our results showed that the risk score was negatively related to immunoglobulin G and LCK (Figure 6H) indicating suppressed T-cell function and B-cell function in high-risk patients.

The correlation between the risk score and various immune biomarkers was analyzed.[18,19] High-risk patients had significantly greater levels of subclonal neo-antigens, suggesting a lower likelihood of responding to immunotherapy (Figure 6I). Signatures of the T-cell dysfunction, exclusion, and TIDE score that integrate T-cell dysfunction and exclusion[18] were also evaluated. As expected, the high-risk group had significantly higher T-cell exclusion and TIDE scores (Figure 6J), suggesting crippled T-cell function. These results suggest that the IL–based signature is a potential candidate for immunotherapy, and the high-risk group may respond poorly to it.

Discussion

The correlation between the IL family and CAFs infiltration and prognosis in PC has not been studied yet. This study systematically analyzed the relationship between IL family expression, CAFs infiltration and PC prognosis for the first time. We demonstrated that increased CAFs and apCAFs correlate with IL family expression patterns. The first IL family expression pattern for predicting CAFs infiltration, spatial distribution, immunotherapy response and PC patient prognosis was constructed.

CAFs are the main non-tumor component of the tumor microenvironment in PC and have been reported to contribute to cancer progression and poor immunotherapy responses.[20] CAFs prevent CD8 T-cell infiltration in tumors,[21] and recruit immunosuppressive cells including myeloid-derived suppressor cells and neutrophils. ApCAF enhances Treg-mediated immunosuppression while iCAF with an inflammatory phenotype secrete tumor-promoting cytokines.[22,23] The infiltration level of apCAFs can serve as a predictor of the immune therapy response, highlighting its significant value in clinical

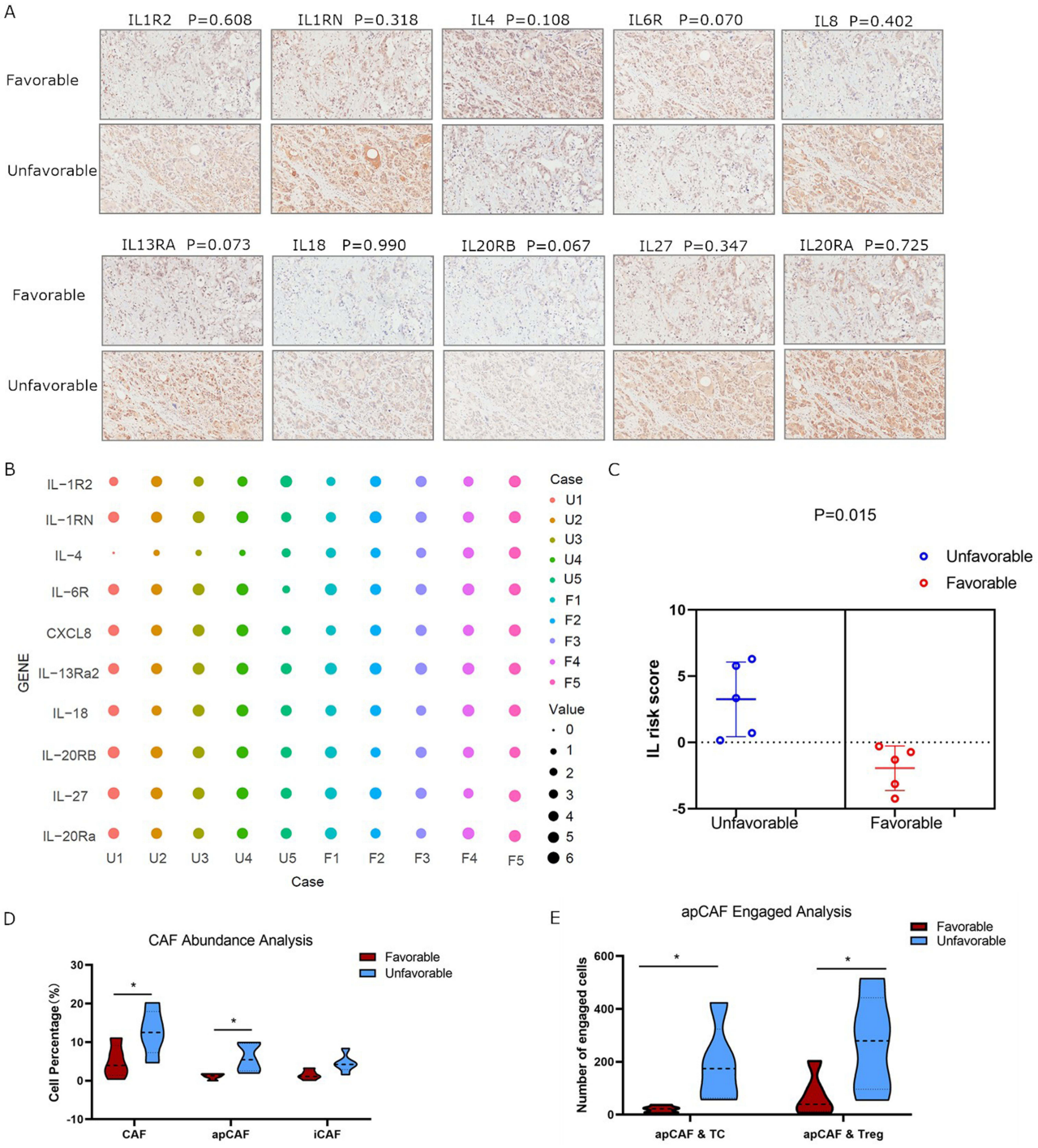

Figure 5 IL expression pattern and immune cell infiltration signature in PC patients with favorable or unfavorable response to immunotherapy. (**A**) IL family expression analysis in PC patients with favorable (n = 5) and unfavorable (n = 5) responses to immunotherapy. Representative pictures are shown. (**B**) IL family expression scores of patients with favorable and unfavorable immunotherapy responses. Individual patients are shown. U, unfavorable; F, Favorable. (**C**) IL risk scores for patients with favorable or unfavorable responses. (**D**) CAF abundance in tumor tissues of patients with favorable and unfavorable responses. (**E**) Number of highly engaged apCAFs and TC/ Tregs in tumor tissues of patients with favorable and unfavorable response. TC, epithelial tumor cells. *, p<0.05.

applications. Targeting specific CAF subtypes in combination with immunotherapy may emerge as a promising strategy to enhance patient response.[24,25]

Tumor heterogeneity leads to region-specific and cell type-dependent expression patterns of IL family members. Metastatic foci often exhibit elevated expression levels of pro-metastatic and immunosuppressive interleukins.[26–28]

https://doi.org/10.2147/JIR.S532651

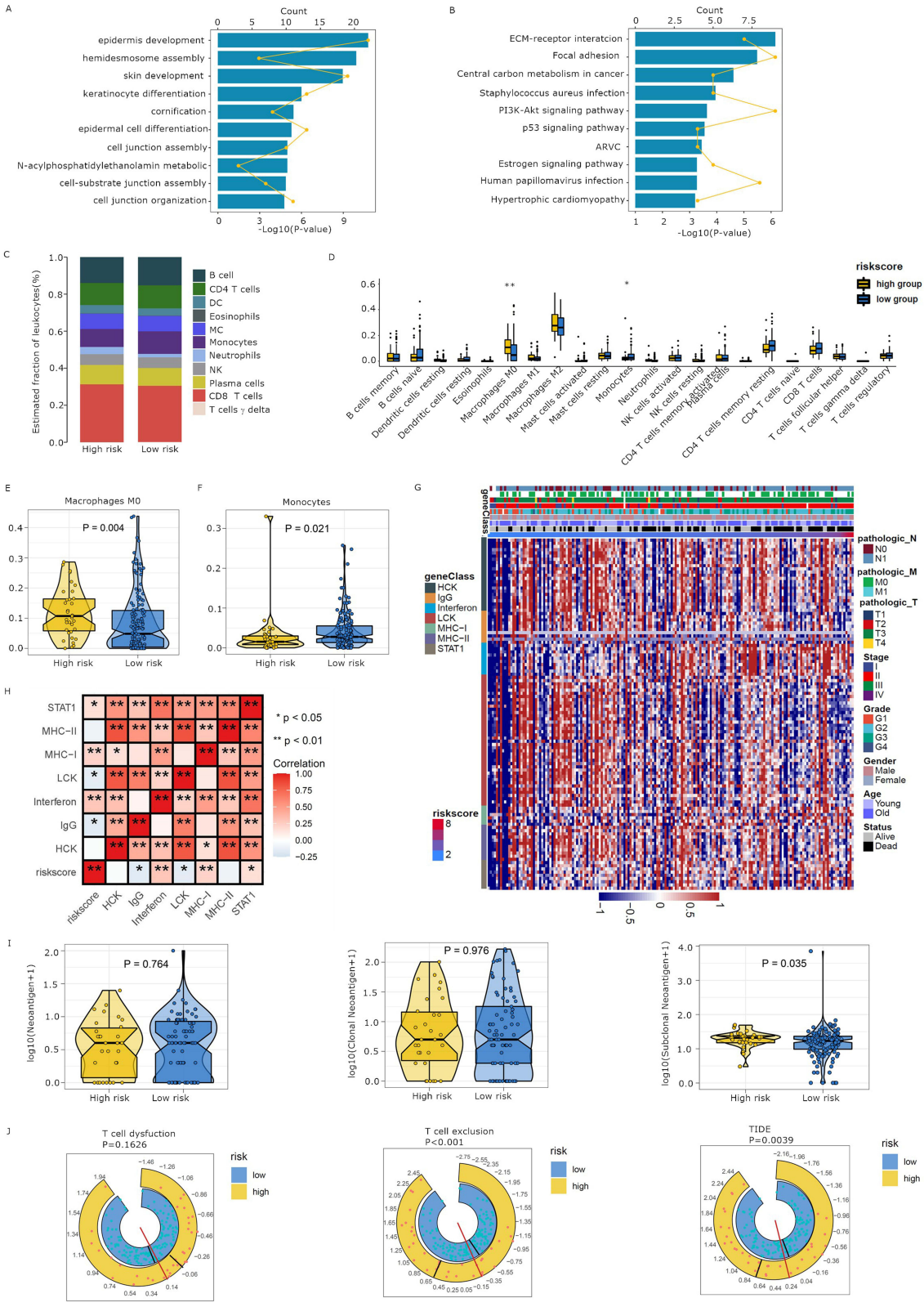

Figure 6 Immune signature and immunotherapy response of the IL family–based signature in PAAD. (**A**) GO and KEGG (**B**) analysis of differentially expressed genes of the IL family–based risk scores. (**C**) Distribution of estimated immune cells in the high- and low-risk groups in the TCGA cohort. (**D**) Differences in the proportions of 22 distinct immune cell subtypes between risk groups. (**E**) Distribution of M0 macrophages and (**F**) monocytes in the high- and low-risk groups. (**G**) Association between risk score and immune response genes. (**H**) Correlogram risk score vs immune system–related metagenes using Pearson's R-value. * and ** represent $p < 0.05$ and $p < 0.01$, respectively. (**I**) Distribution of the number of neo-antigens, clonal neo-antigens, and subclonal neo-antigens in the high- and low-risk groups. (**J**) The distribution of T-cell dysfunction score, T-cell exclusion score, and TIDE score in the high- and low-risk groups.

However, the current understanding of the dynamic regulatory network of the IL family within the tumor microenvironment remains limited.

Members of the interleukin (IL) family (such as IL-8) may serve as potential predictive markers for immunotherapy response. However, the predictive reliability is affected by cancer type, detection methods, and differences among patient populations.[29] In addition, the predictive ability of a single IL marker is usually limited and it is difficult to comprehensively reflect the complex immune response mechanism.

There are complex interactions between the IL family and the activation and differentiation of cancer-associated fibroblasts (CAFs). CAF activation is induced by various stimuli, including IL-6.[30] CAFs affect cytokine and chemokine production, such as IL-1β, IL-6/8 and CXCL12.[31,32] The IL-1-induced signaling cascade leads to JAK/STAT activation, promoting an iCAF state in PDAC.[5] Binding of IL-1β to IL1R1 on fibroblasts activates the NF-κB and JNK pathways, inducing a transcriptional program that drives iCAF differentiation.[33] Treg-derived IL1R2 inhibits IL-1 signaling in CAFs, enhancing MHC-II expression and apCAF functionality.[34]

IL-6 prevents CD8 T-cell infiltration in tumors,[35] mediates crosstalk between CAFs and tumor cells by supporting tumor growth and fibroblast activation.[36] IL-6 also promotes immunosuppression via reprograms metabolism.[37]

IL-17A-producing $CD8^+$ T cells promote PDAC by inducing inflammatory CAFs.[38]

ILs also play a critical role in the development and progression of PC.[6] For the first time, the current study systematically analyzed the relationship between IL family expression and the prognosis of PC.

A signature based on 10 IL(R)s including *IL18, IL20RA, IL20RB, IL6R, IL1RN, IL1R2, CXCL8, IL4, IL27*, and *IL13RA2* was constructed using TCGA PAAD dataset. The signature effectively distinguished patient prognosis in clinical samples. We also evaluated the IL risk signature and prognosis in GEO and ICGC datasets. Given the limitation of relatively small sample sizes in individual databases, we employed a prognostic meta-analysis to further validate the robustness of the IL risk signature model in predicting the prognosis of PDAC patients.

IL18 is associated with T-cell exhaustion.[39] *IL20RA, IL20RB, IL1RN, IL1R2*, and *CXCL8* were reported to promote carcinogenesis.[40] *IL20* blockade promotes CD8+ T-cell infiltration and inhibits tumor growth in PC.[41] *IL1R2* and *IL1RN* correlate positively with immune checkpoint gene expression. IL-4, IL-13, and IL-27, are pleiotropic cytokines with diverse immune functions.[42] Both pro- and anti-tumorigenic roles have been suggested for IL-4 and IL-27 in PC.[43,44] Overexpression of the IL-13Rα2 profoundly inhibited PC tumor development in immunodeficient animals.[45] Our study suggested that *IL27, IL1RN, IL1R2, IL18, IL20RB, IL20RA*, and *CXCL8* are risk factors, while *IL4, IL13RA2*, and *IL6R* are protective factors for PC.

The clinical analysis revealed that IL signature is an independent prognosis-related risk factor for PC patients. Patients in the IL high-risk group exhibit advanced tumors, lymph node metastasis, and increased tumor cell proliferation. Both p53 mutations and high PD-L1 expression are considered to be poor prognostic factors in PC.[46,47] As anticipated, patients in the high-risk group had significantly high rates of p53 mutations and elevated PD-L1 expression in tumor tissues. The current study also showed that genes that are closely related to IL risk scores are enriched in focal adhesion, p53, and PI3K/Akt pathway, which are important for proliferation, metastasis, and chemoresistance in PC.

Our study also evaluated the CAF component's impact on PC prognosis. Here, we used TSA multiplex immunophenotyping to assess the CAF infiltration in PC stroma. We found for the first time that increased CAFs and apCAFs frequencies correlate with poorer prognosis in PC. Infiltration level of apCAFs also correlates with Tregs level.

Immune function relies on cell-to-cell contact and short-distance cytokine communication. The proximity of the tumor to immune cells correlates with its aggressiveness and treatment response.[48,49] However, the correlation between the proximity of the tumor to CAFs or immune cells to CAFs has never been explored. For the first time, our research reveals that the spatial distribution of apCAFs close to tumor cells is associated with shortened survival in PC. We further showed for the first time that high engagement between apCAFs and Tregs in tumor tissues correlates with an unfavorable PC prognosis.

In this study, patients in the IL-based high-risk group showed significantly higher infiltration rates of CAFs, apCAFs, and iCAFs in tumor samples, indicating that the IL signature effectively distinguishes CAF infiltration. In our cohort, PC patients with a favorable response to immunotherapy had significantly lower IL risk score than those with unfavorable responses suggesting predictive power for immunotherapy response. Furthermore, the high-risk group exhibited

significantly higher levels of apCAF / tumor cell, and apCAF /Tregs engagement in the tumor microenvironment, further confirming the IL family signature can predict the immunotherapy response in PC.

The immune profile related to the IL family–based signature was explored. The high-risk group had significantly fewer monocytes and more M0 macrophages. Patients in the high-risk group featured suppressed T-cell function and B-cell function, highlighting an immunosuppressive landscape in these patients. Recent studies emphasize the role of innate immune cells like monocytes in tumor progression. Monocytes exert anti-tumor effects in PC by degrading tumor fibrosis while tumor-associated macrophages promote tumor progression through immunosuppression.[50,51] B-cells in tertiary lymphatic structures are related to better immunotherapy responses.[52,53] Our results suggest that patients in the high-risk group may experience immunosuppression and poorer immunotherapy outcomes.

The role of the IL family–based signature in immunotherapy response was further evaluated using widely adopted biomarkers. TIDE score, a more accurate biomarker for ICB response than traditional ones,[18] and subclonal neo-antigens, which indicate lower likelihood of immunotherapy response when present in high proportions,[54] were analyzed. The current study showed that the high-risk group had significantly higher TIDE scores and levels of subclonal neo-antigens, suggesting the IL-based signature can predict immunotherapy response in PC.

In conclusion, the current study constructed the first IL family expression signature correlated with the prognosis of PC patients, CAFs characteristics, and immune response. These novel findings suggest the potential of the IL family–based signature as a related factor for prognosis and immunotherapy response in PC. To our knowledge, this is the first and most comprehensive analysis of IL expression pattern related to CAFs infiltration, immunotherapy response, and prognosis in PC patients, promoting precise immunotherapy application and treatment options. We will further evaluate the role of IL risk score in prognostic evaluation and prediction of immunotherapy response within a larger clinical cohort. A prospective study to analyze the relationship between the expression pattern of serum IL and prognosis in patients is also warranted. Additionally, we will investigate the specific molecular mechanisms through which the IL family regulate the immunotherapy response.

Ethics Statement

The study was approved by the Ethics Committee of Nanfang Hospital, Southern Medical University.

Consent for Publication

All authors critically reviewed and approved the final manuscript.

Informed Consent

Each patient provided their informed consent in writing, allowing use of samples and clinical data.

Funding

This work was supported by the National Natural Science Foundation of China (no. 82473012 & 82073174), Foundation for Basic and Applied Basic Research of Guangdong Province (no. 2022A1515012406 & 2024A1515030242).

Disclosure

The authors declare that they have no conflicts of interest. This paper has been uploaded to ResearchSquare as a preprint: https://www.researchsquare.com/article/rs-3963463/v1.

References

1. Siegel RL, Miller KD, Jemal A. Cancer statistics, 2019. *CA Cancer J Clin*. 2019;69(1):7–34.
2. Taieb J, Prager GW, Melisi D, et al. First-line and second-line treatment of patients with metastatic pancreatic adenocarcinoma in routine clinical practice across Europe: a retrospective, observational chart review study. *ESMO Open*. 2020;5(1):e000587. doi:10.1136/esmoopen-2019-000587
3. Schumacher TN, Schreiber RD. Neoantigens in cancer immunotherapy. *Science*. 2015;348(6230):69–74. doi:10.1126/science.aaa4971
4. Kabacaoglu D, Ciecielski KJ, Ruess DA, et al. Immune Checkpoint Inhibition for Pancreatic Ductal Adenocarcinoma: current Limitations and Future Options. *Front Immunol*. 2018;9:1878. doi:10.3389/fimmu.2018.01878

5. Vaish UA-OX, Jain T, Are AC, et al. Cancer-Associated Fibroblasts in Pancreatic Ductal Adenocarcinoma: an Update on Heterogeneity and Therapeutic Targeting. *International Journal of Molecular Sciences*. 2021;22(24):13408. doi:10.3390/ijms222413408
6. Briukhovetska D, et al. Interleukins in cancer: from biology to therapy. *Nat Rev Cancer*. 2021;21(1):1–19. doi:10.1038/s41568-020-00319-9
7. Chen X, Tian J, Su GH, et al. Blocking IL-6/GP130 Signaling Inhibits Cell Viability/Proliferation, Glycolysis, and Colony Forming Activity in Human Pancreatic Cancer Cells. *Curr Cancer Drug Targets*. 2019;19(5):417–427. doi:10.2174/1568009618666180430123939
8. Verma G, Bhatia H, Datta M. Gene expression profiling and pathway analysis identify the integrin signaling pathway to be altered by IL-1β in human pancreatic cancer cells: role of JNK. *Cancer Lett*. 2012;320(1):86–95. doi:10.1016/j.canlet.2012.01.036
9. Bellone G, Smirne C, Mauri FA, et al. Cytokine expression profile in human pancreatic carcinoma cells and in surgical specimens: implications for survival. *Cancer Immunol Immunother*. 2006;55(6):684–698. doi:10.1007/s00262-005-0047-0
10. Cheng Y, Wang K, Geng L, et al. Identification of candidate diagnostic and prognostic biomarkers for pancreatic carcinoma. *EBioMedicine*. 2019;40:382–393.
11. Köbel M, Ronnett BM, Singh N, et al. Interpretation of P53 Immunohistochemistry in Endometrial Carcinomas: toward Increased Reproducibility. *Int J Gynecol Pathol*. 2019;38(1):S123–31. doi:10.1097/PGP.0000000000000488
12. Cheng Y, Zheng H, Wang B, et al. Sorafenib and fluvastatin synergistically alleviate hepatic fibrosis via inhibiting the TGFβ1/Smad3 pathway. *Digestive and Liver Disease*. 2018;50(4):381–388. doi:10.1016/j.dld.2017.12.015
13. Gentles AJ, Newman AM, Liu CL, et al. The prognostic landscape of genes and infiltrating immune cells across human cancers. *Nat Med*. 2015;21(8):938–945. doi:10.1038/nm.3909
14. Charoentong P, Finotello F, Angelova M, et al. Pan-cancer Immunogenomic Analyses Reveal Genotype-Immunophenotype Relationships and Predictors of Response to Checkpoint Blockade. *Cell Rep*. 2017;18(1):248–262. doi:10.1016/j.celrep.2016.12.019
15. Maestri EA-O, Kedei N, Khatib S, et al. Spatial proximity of tumor-immune interactions predicts patient outcome in hepatocellular carcinoma. *Hepatology*. 2024;79(4):768–779. doi:10.1097/HEP.0000000000000600
16. Rody A, Holtrich U, Pusztai L, et al. T-cell metagene predicts a favorable prognosis in estrogen receptor-negative and HER2-positive breast cancers. *Breast Cancer Res*. 2009;11(2):R15. doi:10.1186/bcr2234
17. Hänzelmann S, Castelo R, Guinney J. GSVA: gene set variation analysis for microarray and RNA-seq data. *BMC Bioinf*. 2013;14(1):7. doi:10.1186/1471-2105-14-7
18. Jiang P, Gu S, Pan D, et al. Signatures of T cell dysfunction and exclusion predict cancer immunotherapy response. *Nat Med*. 2018;24(10):1550–1558. doi:10.1038/s41591-018-0136-1
19. Nishino M, Ramaiya NH, Hatabu H, et al. Monitoring immune-checkpoint blockade: response evaluation and biomarker development. *Nat Rev Clin Oncol*. 2017;14(11):655–668. doi:10.1038/nrclinonc.2017.88
20. Chakravarthy A, Khan L, Bensler NP, et al. TGF-β-associated extracellular matrix genes link cancer-associated fibroblasts to immune evasion and immunotherapy failure. *Nature Communications*. 2018;9(1). doi:10.1038/s41467-018-06654-8.
21. Salmon H, Franciszkiewicz K, Damotte D, et al. Matrix architecture defines the preferential localization and migration of T cells into the stroma of human lung tumors. *Journal of Clinical Investigation*. 2012;122(3):899–910. doi:10.1172/JCI45817
22. Öhlund DA-O, Handly-Santana A, Biffi G, et al. Distinct populations of inflammatory fibroblasts and myofibroblasts in pancreatic cancer. *Journal of Experimental Medicine*. 2017;214(3):579–596. doi:10.1084/jem.20162024
23. Biffi G, Oni TE, Spielman B, et al. IL1-Induced JAK/STAT Signaling Is Antagonized by TGFβ to Shape CAF Heterogeneity in Pancreatic Ductal Adenocarcinoma. *Cancer Discovery*. 2019;9(2):282–301. doi:10.1158/2159-8290.CD-18-0710
24. Song J, Wei R, Liu C, et al. Antigen-presenting cancer associated fibroblasts enhance antitumor immunity and predict immunotherapy response. *Nature Communications*. 2025;16(1). doi:10.1038/s41467-025-57465-7.
25. Feng B, Wu J, Shen B, et al. Cancer-associated fibroblasts and resistance to anticancer therapies: status, mechanisms, and countermeasures. *Cancer Cell International*. 2022;22(1). doi:10.1186/s12935-022-02599-7.
26. Sadik A, Somarribas Patterson LF, Öztürk S, et al. IL4I1 Is a Metabolic Immune Checkpoint that Activates the AHR and Promotes Tumor Progression. *Cell*. 2020;182(5):1252–1270.e34. doi:10.1016/j.cell.2020.07.038
27. Xie S, Cai Y, Chen D, et al. Single-cell transcriptome analysis reveals heterogeneity and convergence of the tumor microenvironment in colorectal cancer. *Frontiers in Immunology*. 2023;13. doi:10.3389/fimmu.2022.1003419
28. Angerilli V, Callegarin M, Govoni I, et al. Heterogeneity of predictive biomarker expression in gastric and esophago-gastric junction carcinoma with peritoneal dissemination. *Gastric Cancer*. 2025;28(4):569–578. doi:10.1007/s10120-025-01609-7
29. Schalper KA-O, Carleton M, Zhou M, et al. Elevated serum interleukin-8 is associated with enhanced intratumor neutrophils and reduced clinical benefit of immune-checkpoint inhibitors. *Nature Medicine*. 2020;26(5):688–692. doi:10.1038/s41591-020-0856-x
30. Santi A, Kugeratski FG, Zanivan S. Cancer Associated Fibroblasts: the Architects of Stroma Remodeling. *PROTEOMICS*. 2018;18(5–6). doi:10.1002/pmic.201700167
31. Feig C, Jones JO, Kraman M, et al. Targeting CXCL12 from FAP-expressing carcinoma-associated fibroblasts synergizes with anti-PD-L1 immunotherapy in pancreatic cancer. *Proceedings of the National Academy of Sciences*. 2013;110(50):20212–20217. doi:10.1073/pnas.1320318110
32. Han Y, Zhang Y, Jia T, et al. Molecular mechanism underlying the tumor-promoting functions of carcinoma-associated fibroblasts. *Tumor Biology*. 2015;36(3):1385–1394. doi:10.1007/s13277-015-3230-8
33. Koncina EA-O, Nurmik M, Pozdeev VI, et al. IL1R1(+) cancer-associated fibroblasts drive tumor development and immunosuppression in colorectal cancer. *Nature Communications*. 2023;14(1). doi:10.1038/s41467-023-39953-w.
34. Chen L, Huang H, Zheng X, et al. IL1R2 increases regulatory T cell population in the tumor microenvironment by enhancing MHC-II expression on cancer-associated fibroblasts. *Journal for ImmunoTherapy of Cancer*. 2022;10(9):e004585. doi:10.1136/jitc-2022-004585
35. Monteran L, Erez N. The Dark Side of Fibroblasts: cancer-Associated Fibroblasts as Mediators of Immunosuppression in the Tumor Microenvironment. *Frontiers in Immunology*. 2019;10. doi:10.3389/fimmu.2019.01835
36. Karakasheva TA, Lin EW, Tang Q, et al. IL-6 Mediates Cross-Talk between Tumor Cells and Activated Fibroblasts in the Tumor Microenvironment. *Cancer Research*. 2018;78(17):4957–4970. doi:10.1158/0008-5472.CAN-17-2268
37. Flint TR, Janowitz T, Connell C, et al. Tumor-Induced IL-6 Reprograms Host Metabolism to Suppress Anti-tumor Immunity. *Cell Metabolism*. 2016;24(5):672–684. doi:10.1016/j.cmet.2016.10.010

38. Picard FA-O, Lutz V, Brichkina A, et al. IL-17A-producing CD8 + T cells promote PDAC via induction of inflammatory cancer-associated fibroblasts. *Gut*. 2023;72(8):1510–1522. doi:10.1136/gutjnl-2022-327855
39. Ahmed A, Klotz R, Köhler S, et al. Immune features of the peritumoral stroma in pancreatic ductal adenocarcinoma. *Front Immunol*. 2022;13:947407. doi:10.3389/fimmu.2022.947407
40. Dumoutier L, Leemans C, Lejeune D, et al. Cutting edge: STAT activation by IL-19, IL-20 and mda-7 through IL-20 receptor complexes of two types. *J Immunol*. 2001;167(7):3545–3549. doi:10.4049/jimmunol.167.7.3545
41. Lu SW, Pan H-C, Hsu Y-H, et al. IL-20 antagonist suppresses PD-L1 expression and prolongs survival in pancreatic cancer models. *Nat Commun*. 2020;11(1):4611. doi:10.1038/s41467-020-18244-8
42. Shi J, Song X, Traub B, et al. Involvement of IL-4, IL-13 and Their Receptors in Pancreatic Cancer. *Int J Mol Sci*. 2021;22(6):2998. doi:10.3390/ijms22062998
43. Kwaśniak K, Czarnik-Kwaśniak J, Maziarz A, et al. Scientific reports concerning the impact of interleukin 4, interleukin 10 and transforming growth factor β on cancer cells. *Cent Eur J Immunol*. 2019;44(2):190–200. doi:10.5114/ceji.2018.76273
44. van Duijneveldt G, Griffin MDW, Putoczki TL. Emerging roles for the IL-6 family of cytokines in pancreatic cancer. *Clin Sci*. 2020;134(16):2091–2115. doi:10.1042/CS20191211
45. Kawakami K, Kawakami M, Snoy PJ, et al. In vivo overexpression of IL-13 receptor alpha 2 chain inhibits tumorigenicity of human breast and pancreatic tumors in immunodeficient mice. *J Exp Med*. 2001;194(12):1743–1754. doi:10.1084/jem.194.12.1743
46. Iwatate Y, Hoshino I, Yokota H, et al. Radiogenomics for predicting p53 status, PD-L1 expression, and prognosis with machine learning in pancreatic cancer. *Br J Cancer*. 2020;123(8):1253–1261. doi:10.1038/s41416-020-0997-1
47. Hu Y, Zha Y, Kong F, et al. Prognostic value of PD-L1 expression in patients with pancreatic cancer: a PRISMA-compliant meta-analysis. *Medicine*. 2019;98(3):e17432. doi:10.1097/MD.0000000000017432
48. Carstens JL, Correa de Sampaio P, Yang D, et al. Spatial computation of intratumoral T cells correlates with survival of patients with pancreatic cancer. *Nat Commun*. 2017;8(1). doi:10.1038/ncomms15095.
49. Tsujikawa T, Mitsuda J, Ogi H, et al. Prognostic significance of spatial immune profiles in human solid cancers. *Cancer Sci*. 2020;111(10):3426–3434. doi:10.1111/cas.14591
50. Long KB, Gladney WL, Tooker GM, et al. IFNγ and CCL2 Cooperate to Redirect Tumor-Infiltrating Monocytes to Degrade Fibrosis and Enhance Chemotherapy Efficacy in Pancreatic Carcinoma. *Cancer Discov*. 2016;6(4):400–413. doi:10.1158/2159-8290.CD-15-1032
51. Pucci M, Raimondo S, Urzì O, et al. Tumor-Derived Small Extracellular Vesicles Induce Pro-Inflammatory Cytokine Expression and PD-L1 Regulation in M0 Macrophages via IL-6/STAT3 and TLR4 Signaling Pathways. *Int J Mol Sci*. 2021;22(22):12118. doi:10.3390/ijms222212118
52. Kang W, Feng Z, Luo J, et al. Tertiary Lymphoid Structures in Cancer: the Double-Edged Sword Role in Antitumor Immunity and Potential Therapeutic Induction Strategies. *Front Immunol*. 2021;12. doi:10.3389/fimmu.2021.689270
53. Jacquelot N, Tellier J. Tertiary lymphoid structures and B lymphocytes in cancer prognosis and response to immunotherapies. *Oncoimmunology*. 2021;10(1):1900508.
54. McGranahan N, Furness AJS, Rosenthal R, et al. Clonal neoantigens elicit T cell immunoreactivity and sensitivity to immune checkpoint blockade. *Science*. 2016;351(6280):1463–1469. doi:10.1126/science.aaf1490